Kinematics of the Vatyn–Lesnaya Thrust Fault (Southern Koryakia)

A. V. Solov'ev*, M. T. Brandon**, J. I. Garver***, and M. N. Shapiro****

*Institute of the Lithosphere of Marginal Seas, Russian Academy of Sciences, Staromonetnyi per. 22, Moscow, 109180 Russia
**Yale University, 210 Whitney Avenue, P.O. Box 208109, New Haven, US
***Union College, Schenectady NY, 12308-2311, US
****Schmidt Joint Institute of Physics of the Earth, Russian Academy of Sciences,
Bol'shaya Gruzinskaya ul. 10, Moscow, 123810 Russia
Received May 15, 2000

Abstract—The Vatyn–Lesnaya thrust fault, exposed in southern Koryakia and northern Kamchatka, is among the largest collisional sutures in northeast Asia. The thrust fault juxtaposes the terrane of a Pacific island-arc system against the deposits of the Eurasian continental margin. Thrusting terminated the arc–continent collision in the Middle Eocene. Based on a detailed structural analysis, the structure and kinematics of the suture zone were deduced and its evolution model was compiled. An attempt to discriminate structural features by age is presented. The origin of structural features is interpreted against the background of the region-scale of Late Mesozoic–Cenozoic geodynamics.

INTRODUCTION

The Vatyn–Lesnaya thrust fault is among the largest sutures in northeast Asia, traceable over more than 800 km in southern Koryakia and Northern Kamchatka [15, 19, 28, 31, 33]. The suture separates the Cretaceous–Paleogene deposits of the Eurasian continental margin [5, 11, 18, 21, 28] from the marginal marine and island-arc assemblages of the Cretaceous–Paleocene age [5, 30], which were formed in the Pacific and transported over considerable distances [13, 14]. The flyschoid sequence of the continental margin presently occurs in the Ukelayat–Lesnaya trough [11, 18, 21, 28], whereas the marginal marine and island-arc assemblages occur in the Olyutorsky zone with a mosaic heterogeneous basement [6].

The models of collision between the Cretaceous island-arc system and the Eurasian continental margin proposed by our predecessors were based on geologic [16, 18, 30, 32] and paleomagnetic data [13, 32, 40], but the structure and kinematics of the Vatyn–Lesnaya thrust fault have never been taken into account. From 1994–1999, we conducted a detailed study of five domains within the thrust zone (Fig. 1). In each domain, the precise position of the thrust plane was identified, the kinematics of movements on this plane was determined, and the specific structural features of the allochthon and autochthon of the thrust fault zone were studied.

STRUCTURAL ANALYSIS TECHNIQUE

To study the structure of the Vatyn–Lesnaya thrust zone, structural surveys were performed in the autochthonous and allochthonous sequences in the immediate vicinity of the suture, and kinematic indicators on the thrust fault plane were analyzed.

The data on deformations in the autochthon and allochthon are based on field measurements of bedding, cleavage, fault planes, and the orientations of fold axes and axial planes. The hinges of some folds were calculated as β-axes[1] and deduced as π-axes[2] [44]. The stereograms were plotted and the data were analyzed using Spheristat v. 1.1 © Frontenac Wordsmiths (1990) and Quickplot v. 1.0 © D. van Everdingen & J. van Gool (1990) software. Data point densities were contoured using the same method as in [45] and interpreted using the eigenvector method [10, 43].

The directions of the relative displacements along faults (thrust faults) were determined using internal rotation axes analysis [36]. This method is based on the assumption that the symmetry of an ideal fault zone initiated in a setting of progressive simple shear strain is monoclinic (Fig. 2a), i.e., the symmetry of the structural features distribution is monoclinic. The kinematic indicators are mesostructures that bear evidence for the rotational component of deformation such as asymmetrical folds (Fig. 2c) and Riedel structures[3] (Fig. 2b).

---

[1] β-axis is the fold axis (hinge) calculated as a trace of axial planar cleavage on the bedding plane [44].
[2] π-axis is the fold axis (hinge) calculated as being perpendicular to the great-circle girdle, along which the bedding poles are dispersed.
[3] The term Riedel structures is used according to [36] to avoid ambiguity in the names of planar features; in the Russian literature, it corresponds to the term Riedel shear.

(a)

(b)
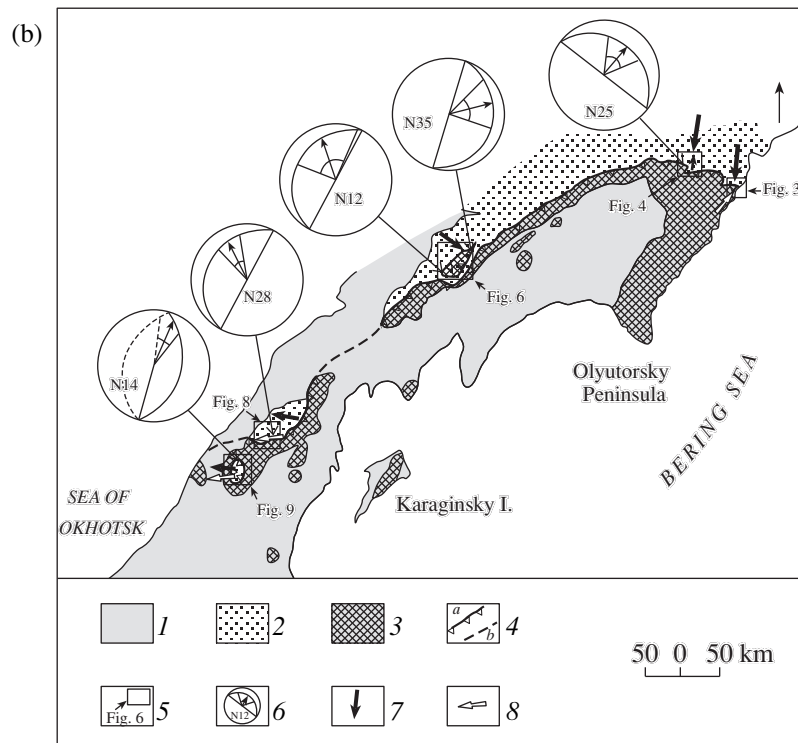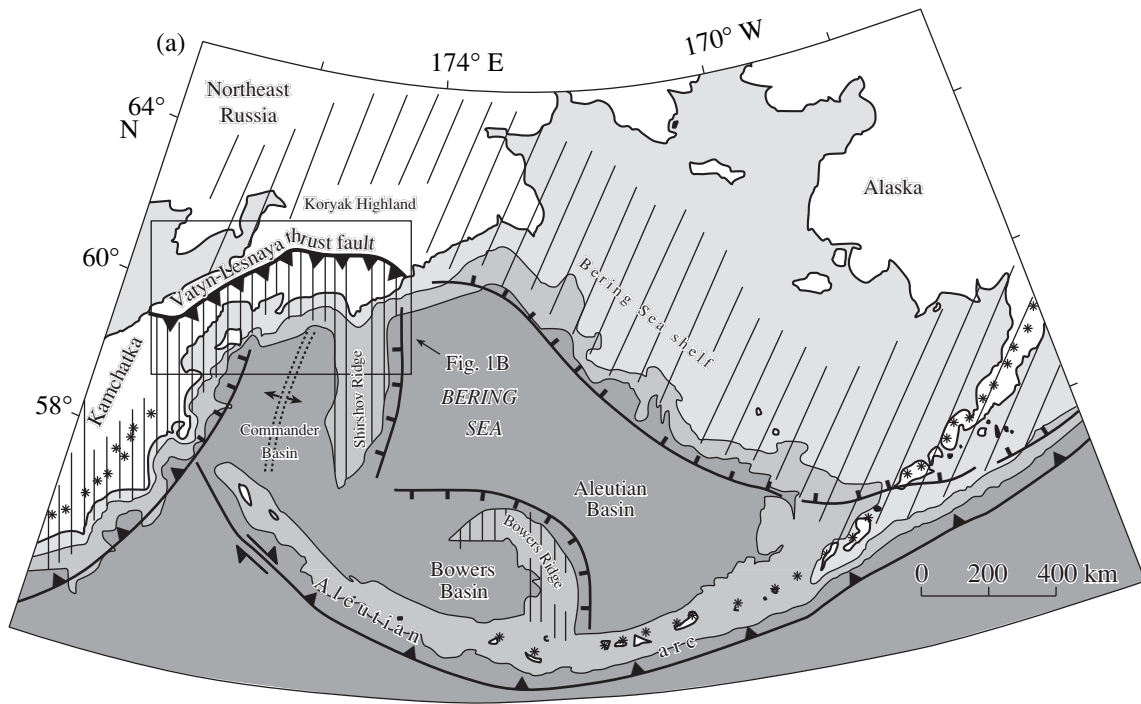
A Riedel structure is an association of planar meso-structures originating from simple shear strain. Experimental studies of Riedel structures suggest that displacements occur along three planes, Y, P, and R, formed in a brittle shear zone; the symmetry of these features, indeed, reflects monoclinic deformation symmetry [42]. A fault zone symmetry plane is deduced from the geometry of structural features observed in this zone, and the intersection of the deduced symmetry plane with the fault plane corresponds to the slip vec-

Fig. 1. Vatyn–Lesnaya thrust fault in the structural framework of the Bering Sea region [15, 27, 28, 35, 48], (a) location; (b) structural–kinematic analysis data. (a): (*1*) Aleutian and Kamchatka arcs with active modern volcanism; (*2*) Olyutorsky–Kamchatka fold zone and its possible offshore extension into the Bering Sea; (*3*) Cretaceous–Paleogene Andean-type marginal volcanic belts initiated on blocks of various ages accreted to Eurasia during the late Mesozoic; (*4*) spreading centers; (*5*) fossil and (*6*) modern trenches; (*7*) Vatyn–Lesnaya thrust fault; (*8*) strike-slip faults. (b): (*1*) Cenozoic deposits undifferentiated; (*2*) clastics of the Ukelayat–Lesnaya thrust (Cretaceous–Eocene); (*3*) volcanic–cherty–clastic deposits of a marginal sea and the Olyutorsky island arc (Cretaceous–Paleocene); (*4*) Vatyn–Lesnaya thrust fault, (*a*) mapped and (*b*) inferred; (*5*) location and number of detailed surveying areas; (*6*) diagrams showing the allochthon slip directions relative to the autochthon in the Vatyn–Lesnaya suture zone derived from the analyses of internal rotation axes on Riedel structures [36]. Wulff net; solid lines indicate projections to the upper hemisphere and dotted lines, to the lower hemisphere. Great-circle girdle corresponds to the average thrust fault orientation in this area. Arrow indicates the synoptic hanging wall slip vector reflecting an average regional tectonic transport durection in the thrust zone; the arc shows the confidence angle. N is the number of structural features (Riedel structures) used in the calculations; (*7*) orientation of the main compression axis during the autochthon structuring event (the flysch filling the Ukelayat–Lesnaya trough), arrows indicate the predominant vergence of the structure; small arrow indicates the vergence near the thrust fault; (*8*) vergence of structures in allochthonous complexes; arrows in the Lesnaya sector of the thrust fault (Figs. 8, 9) indicate the vergence of minor asymmetrical folds (Fig. 11d) widespread in the near-thrust part of the allochthon (Shamanka dome) and between allochthonous slabs (Vatapvayam dome).
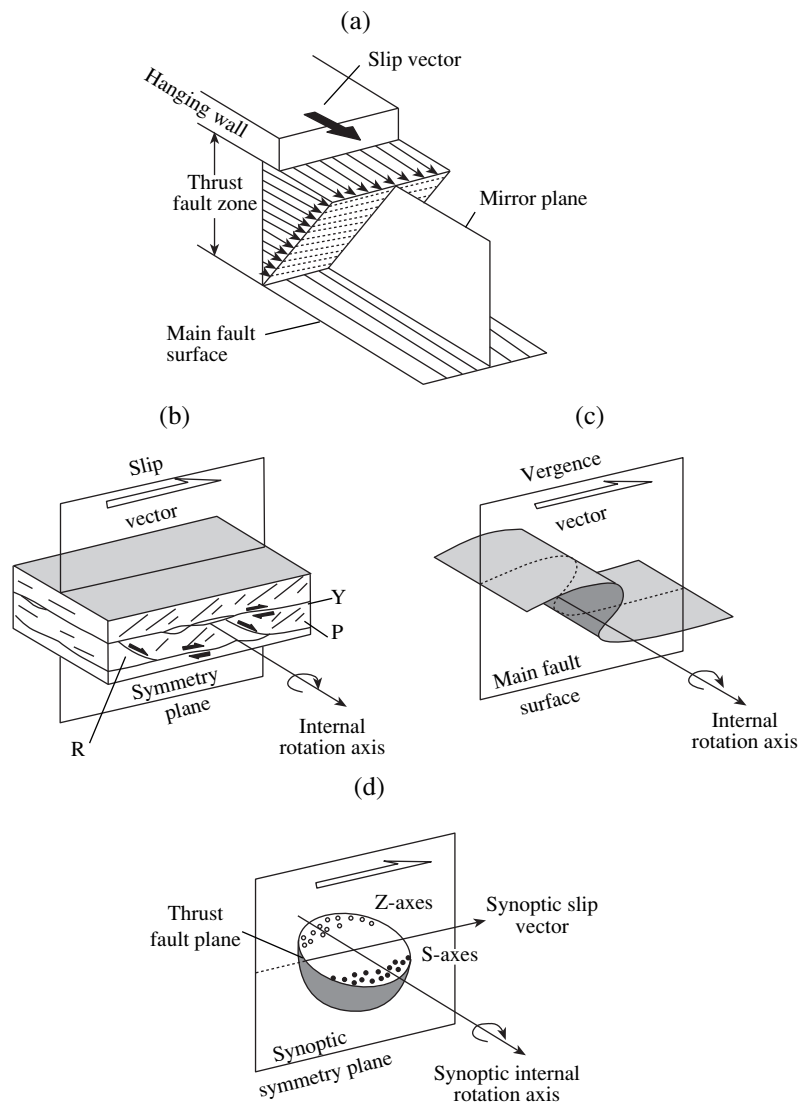
Fig. 2. An ideal scheme of a thrust fault zone with a monoclinic symmetry formed in a setting of progressive non-coaxial deformation [36, 47] (a); internal rotation axes showing the Riedel structure (b) and fold (c) orientations and asymmetry; and a stereogram showing the hypothetical local rotation axes (S and Z) distribution near the average direction called the synoptic rotation axis [36]. For Riedel structures (b): Y—main fault surface, R—secondary splay faults inclined in slip direction (Riedel shears); P—shear joints or cleavage inclined in the opposite direction.

tor—the direction of this vector being interpreted as the slip direction of the hanging wall relative to the footwall. The orientation of any asymmetrical fold or Riedel structure is represented by an internal rotation axis, which indicates the sense of rotation (Figs. 2b, 2c). Rotation is designated as either "S" or "Z" to indicate anticlockwise or clockwise rotation when viewed toward the dip of the axis. The internal rotation axis of an asymmetrical fold is equivalent to the fold axis (Fig. 2c). The internal rotation axis of a Riedel structure is parallel to the trace of a Y-surface on P- or R-surfaces (Fig. 2b). Therefore, internal rotation axes can be calculated from measured Y, P, and R orientations. Hypothetical internal rotation axes distribution in a monoclinic shear zone is shown in Fig. 2d. All axes must lie in the same plane parallel to the fault zone they were formed in. The monoclinic axis distribution symmetry is described by a mirror plane that is perpendicular to the fault plane and bisects the S and Z symmetry groups. The intersection of the mirror plane with the fault surface defines the synoptic hanging wall slip vector. This synoptic vector indicates the average slip direction in modern coordinates. The direction of transport along the fault plane is detected using the following procedure. All S-sense axes of local structures are converted into Z-axes. For example, an S-axis projected onto the upper hemisphere will be mirror-reflected on the lower hemisphere when converted into a Z-axis. Then the Z-transformed axes are projected onto the average fault plane[4] to plot the so-called average fault plane-parallel stereogram. The maximum of Z-transformed axes represents the synoptic rotation axis in the average fault plane, whereas the synoptic (regiona) vector of the hanging wall slip relative to the footwall lies orthogonally in the same plane. The method of determining the mirror plane position and slip vector orientation and the statistical estimates of the defined directions are discussed in [36].

Fault kinematics in stratified flyschoid sequences was studied using the cutoff method [22].

GENERAL STRUCTURE OF THE VATYN–LESNAYA THRUST FAULT AND STRUCTURAL ANALYSIS DATA

The Vatyn–Lesnaya thrust fault is traceable from Anastasia Bay in the northern Olyutorsky zone to the Lesnaya high on the isthmus of the Kamchatka Peninsula (Fig. 1). The upper Cenozoic deposits cover the thrust fault to the north of the Lesnaya high and separate it into two parts, Vatyn–Vyvenka and Lesnaya (Fig. 1b). The northern segment of the thrust fault was described for the first time in the Olyutorsky zone as the Vatyn thrust fault [15]. Later, it was traced farther south on the Kamchatka isthmus, where it was called the Lesnaya thrust fault [31, 33]. The autochthon is com-

posed of the Upper Cretaceous–Middle Eocene flyschoid fill of the Ukelayat–Lesnaya trough [5, 11, 18, 21, 23, 38], on which the Cretaceous marginal marine deposits and the Upper Cretaceous–Paleocene marginal sea and island arc assemblages are obducted [1, 4, 5, 24, 30, 32]. The neoautochthon is only found on the Kamchatka isthmus, and its oldest unit is composed of Middle Eocene subaerial volcanics of the Kinkil' Formation [8].

The autochthon found in the northern Olyutorsky zone **in the vicinity of Anastasia Bay** (Fig. 3) is composed of interbedded sandstone-siltstone–mudstone flysch with occasional gritstones and conglomerates. The allochthonous slices consist of volcanic–cherty and volcaniclastic sequences. The former consists of pillow basalts, hyaloclastites, jasper with inoceramid horizons, cherts, and aleuropelites, whose radiolarian age has been determined as late Turonian–Maastrichtian; the latter consists of basalts, andesites, lava-breccias, tuffs, sandstones, aleuropelites, and cherts and has been dated as Campanian–Maastrichtian [25]. The Vatyn–Lesnaya thrust fault is covered onshore by Quaternary sediments and probably extends offshore across the bay (Fig. 3a).

South of Anastasia Bay, the allochthonous units are deformed into a large synform (Fig. 3b) modified by minor folding; the π-axis of this synform is oriented SE–NW (D1 in Fig. 3a). The flyschoid sequence on the northern side of the bay is deformed into SSW-vergent isoclinal folds (D2 in Fig. 3a; Fig. 3b). The folds in the flysch exhibit axial planar cleavage (D3 in Fig. 3a), and the β-axes of the folds make up one maximum with a northwesterly orientation and a fairly steep inclination (D3 in Fig. 3a). The analysis of all types of structures in the allochthon and autochthon suggests their inception in a SSW–NNE-oriented compression stress field [20].

The flyschoid autochthon **in the Il'pi–Matysken River area** (Fig. 4) exhibits an intensely tectonized sequence of a presumably olistostromic origin at the top. The matrix consists of black aleuropelites with occasional thin sandstone lenses. The blocks are composed of porphyritic and aphyric basalts, lava-breccias, and hyaloclastites of basaltic composition; gabbroids and gabbro-diorites; and scarce black and green cherts. The age of the autochthon near the thrust fault has been determined as late Maastrichtian–Middle Eocene (66.1 ± 6.3 to 43.9 ± 3.6 Ma according to fission-track dating of zircons from sandstones) [21, 38]. The allochthon is composed of pillow basalts, lava-breccias, and hyaloclastites of basaltic composition; jaspers with inoceramid shells; and cherts. Based on radiolarian datings, the allochthon is late Campanian–Maastrichtian in age [24]. In this area, the Vatyn–Lesnaya thrust fault occurs as an imbricated zone with a thickness up to 150 m. This zone is particularly well pronounced on the slopes of the Matysken River valley (Fig. 4a), where it juxtaposes slices of rocks from both the Olyutorsky zone and the Ukelayat trough. The slices are limited by

---

[4] The average fault plane is defined as the great-circle girdle (average girdle) along which the local rotation axes are dispersed.
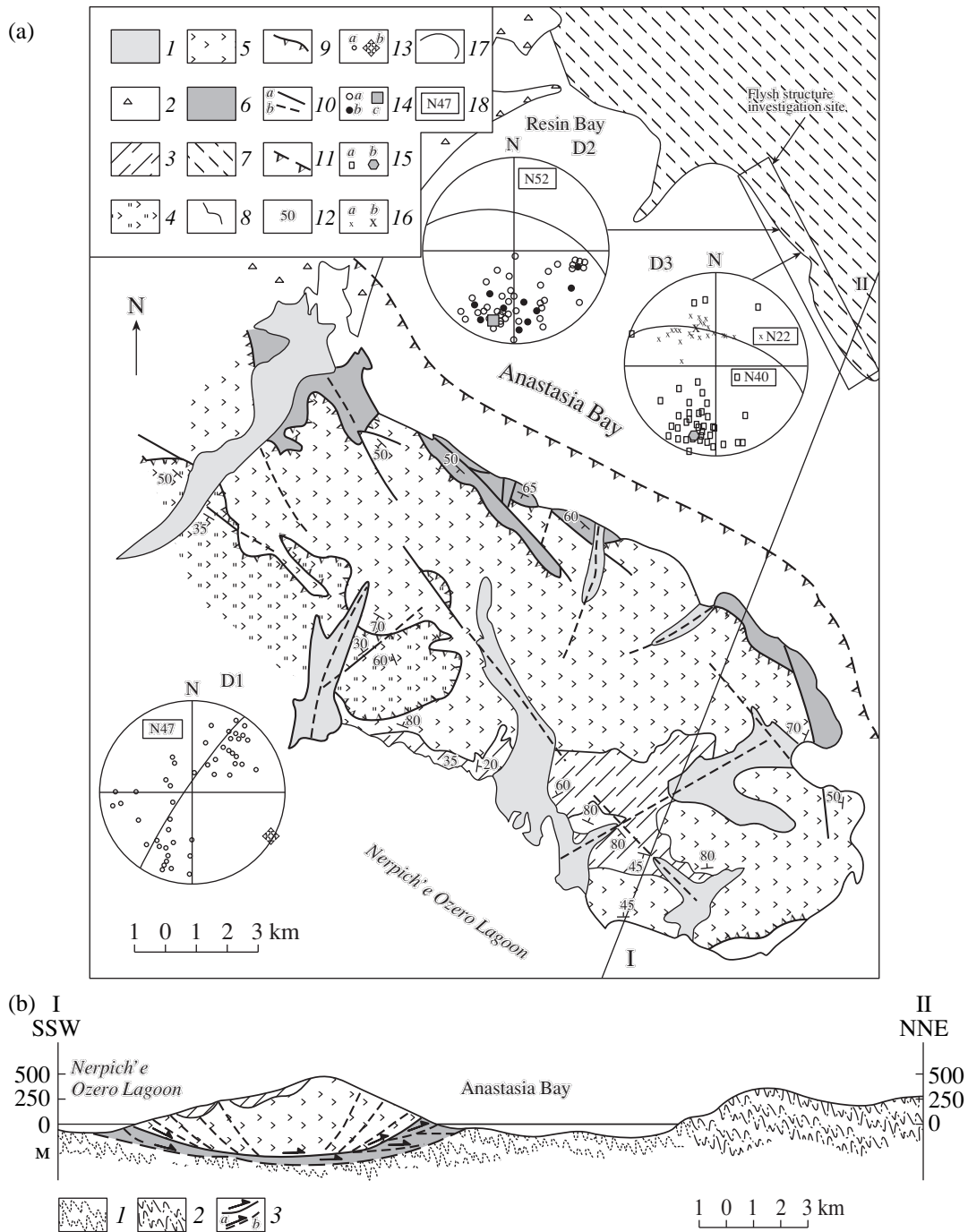
Fig. 3. Geology of the Anastasia Bay area: (a) Geologic map of the Anastasiya Bay area (modified by A.V. Solov'ev, T.N. Palechek and R.M. Palechek after O.V. Astrakhantsev, L.B. Afanas'eva, A.D. Kazimirov, K.A. Krylov, G.V. Polunin, V.I. Aksenov, A.V. Lander, and E.V. Firsova); (b) Schematic cross section. (a): (*1, 2*) Quaternary deposits: (*1*) alluvial and (*2*) marine; (*3–5*) vol-caniclastic deposits (Campanian–Maastrichtian): (*3*) cherti-clastic, (*4*) volcaniclastic, and (*5*) volcanic deposits proper; (*6*) volcanic-cherty deposits (Turonian–Maastrichtian); (*7*) flyschoid deposits of the Ukelayat zone (Cretaceous(?)–Eocene); (*8*) stratigraphic contacts; (*9*) thrust faults; (*10*) high-dipping faults: (*a*) proved and (*b*) inferred; (*11*) the inferred position of the main fault plane of the Vatyn–Lesnaya thrust fault; (*12*) strike and dip symbol. D1, D2, D3 are strereograms of structural features: Schmidt net, projection on the lower hemisphere; (*13*) for the D1 stereogram: *a*—bedding poles; *b*—π-axis of the synform; (*14*) for the D2 diagram: (*a, b*)—bedding poles: (*14a*), with upright and (*14b*), with overturned bedding; *14c*—average pole; (*15, 16*) for the D3 stereogram: (*15a*) cleavage poles, (*15b*) average pole; (*16a*) β-axes of folds; (*16b*) average β-axis; (*17*) great-circle girdles; (*18*) number of structural features included in the analysis. (b): (*1, 2*) structure of flyschoid deposits in the Ukelayat zone: (*1*) inferred, (*2*) proved; (*3*) thrust faults: (*a*) proved, (*b*) inferred. See Fig. 3a for the rest of the legend and Fig. 1b, for location.
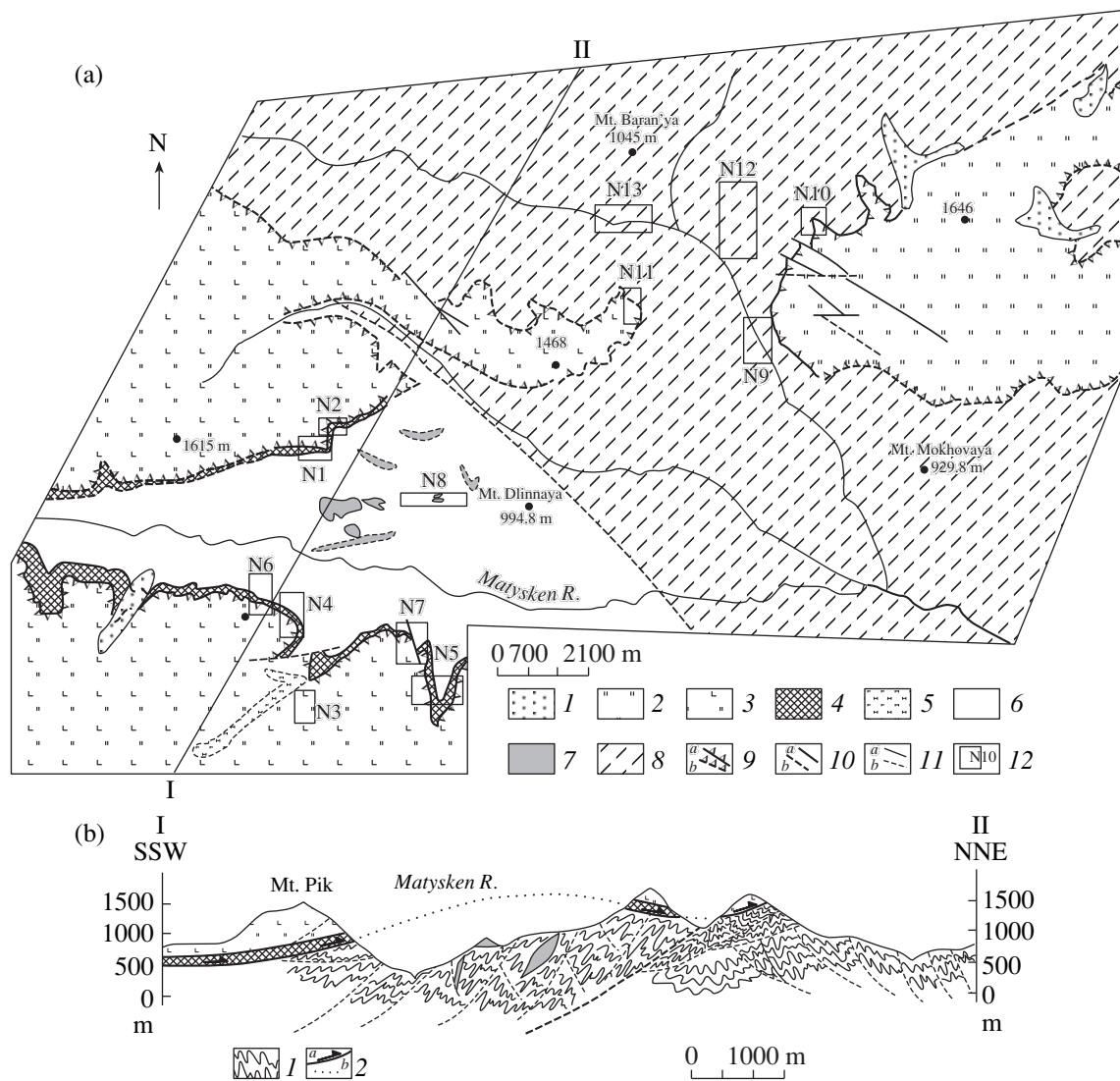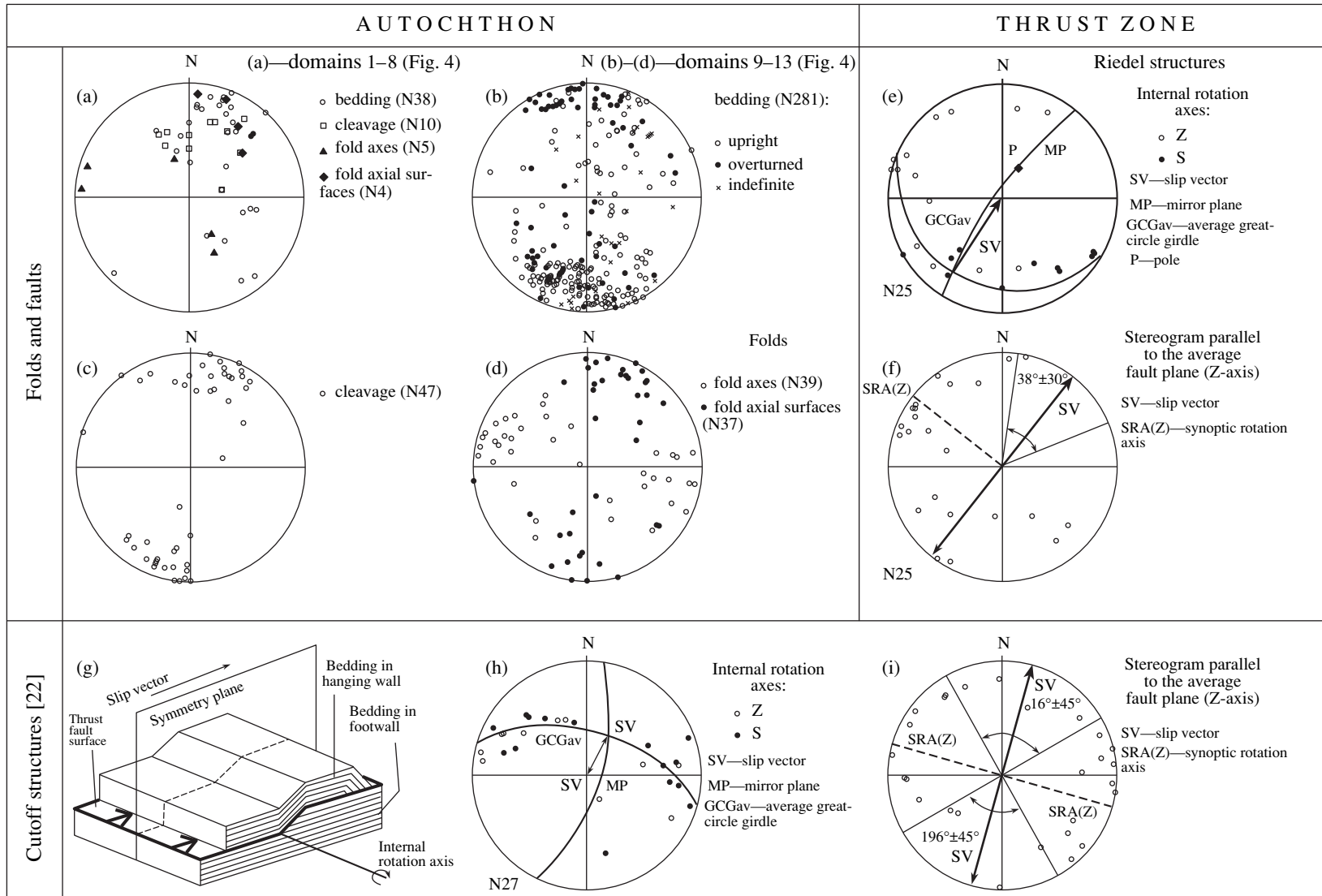
Fig. 4. Geology of the Il'pi and Matysken River headwaters. (a) Geologic map of the Il'pi and Matysken River headwaters. Modified with participation of G.V. Ledneva after A.V. Ditmar, K.S. Ageev, A.S. Finogentov, and E.S. Alekseev; (b) schematic cross section I–II. (a): (*1*) Quaternary deposits; (*2, 3*) volcanic-cherty deposits (Campanian–Maastrichtian): (*2*) cherts and jaspers, (*3*) aphyric pillow basants, cherts, and jaspers; (*4*) Vatyn–Lesnaya thrust fault zone; (*5*) dunite, vehrlite, and clinopyroxenite blocks (Cretaceous–(?)); (*6*) Olistostromic sequence (Paleocene–Middle Eocene); (*7*) basaltoid blocks; (*8*) Ukelayat flysch (Maastrichtian); (*9*) thrust faults: (*a*) proved and (*b*) recognized on the aerial images; (*10*) high-dipping faults: (*a*) proved, (*b*) recognized on the aerial images; (*11*) stratigraphic contacts: (*a*) proved, (*b*) inferred; (*12*) numbers of domains, in which structural surveys were performed. (b): (*1*) folds in the autochthon; (*2*) thrust faults: (*a*) proved, (*b*) inferred eroded thrust surface form. See Fig. 4a for the rest of the legend and Fig. 1b, for location.

subhorizontal sole and roof thrust planes and consist of boudinaged black and green cherts, aphyric basalts and lava breccias, black cataclastic aleuropelites, and occasional fine sandstones. The Vatyn–Lesnaya thrust zone exhibits gentle synforms and antiforms with amplitudes of one- or two-hundred meters and wavelengths of a few kilometers (Fig. 4b).

The autochthon shows a regular distribution of folds with different vergences (Figs. 4a, 4b). The north-northeasterly vergence in the subthrust section of the autochthon (domains 1–8 in Fig. 4a, Fig. 5a) passes into a fanfolding zone and then into a zone with a south-southwestward vergence (domains 9–13 in Fig. 4a, Figs. 5b–5d).

Fold axial planes within domains 9–13 dip both to the north-northeast and south-southwest (Fig. 5d), and the axes strike WNW and ESE with a shallow inclination (Fig. 5d) and axial planar cleavage (Fig. 5c). Cutoff structures are widespread in the autochthonous flysch (Fig. 5g) [22]. The analysis suggests that intraformational thrusting in the flysch sequences was induced by NNE–SSW shortening and was directed both to the south-southwest and the north-northeast (Figs. 5h, 5i). Analysis of Riedel structures in the thrust zone and at the sole of the allochthon in this area suggests that the allochthonous slices were transported northeastward relative to the autochthon (Figs. 5e, 5f).

AUTOCHTHON

THRUST ZONE

Folds and faults

N   (a)—domains 1–8 (Fig. 4)

(a)

○ bedding (N38)
□ cleavage (N10)
▲ fold axes (N5)
◆ fold axial sur-
   faces (N4)

N   (b)–(d)—domains 9–13 (Fig. 4)

(b)

bedding (N281):
○ upright
● overturned
× indefinite

N   Riedel structures

(e)

Internal rotation
axes:
○ Z
● S

SV—slip vector
MP—mirror plane
GCGav—average great-
circle girdle
P—pole

P   MP
GCGav
SV
N25

N

(c)

○ cleavage (N47)

N   Folds

(d)

○ fold axes (N39)
● fold axial surfaces
   (N37)

N   Stereogram parallel
to the average
fault plane (Z-axis)

(f)
SRA(Z)

38°±30°
SV

SV—slip vector
SRA(Z)—synoptic rotation
axis

N25

Cutoff structures [22]

(g)

Slip vector
Symmetry plane
Thrust
fault
surface
Bedding in
hanging wall
Bedding in
footwall
Internal
rotation axis

N

(h)

Internal rotation
axes:
○ Z
● S

SV—slip vector
MP—mirror plane
GCGav—average great-
circle girdle

GCGav
SV
SV   MP
N27

N   Stereogram parallel
to the average
fault plane (Z-axis)

(i)
SV
16°±45°
SRA(Z)

SV—slip vector
SRA(Z)—synoptic rotation
axis

SRA(Z)
196°±45°
SV

Fig. 5. Structural–kinematic analysis data for the Vatyn–Lesnaya thrust fault (Il'pi–Matysken River area, see Fig. 4). (a)–(f) stereograms of structural features: (a) for domains 1–8; (b)–(d) for domains 9–13 (see Fig. 4a): (b) bedding, (c) cleavage, (d) fold axes and axial surfaces; (e) internal rotation axes for Riedel structures; (f) Z-transformed rotation axes for Riedel structures as projected at the average fault plane; (g) idealized ramp model (modified after [46]). The model is adapted for cutoff analysis method enabling fault kinematics to be determined in stratified sequences [22]; (h), (i) stereograms: (h) internal rotation axes for cutoff structures and (i) Z-transformed rotation axes projections on average fault plane. SV—slip vector; the arc shows the confidence angle. Linear and planar features are shown as poles on the Schmidt net, lower hemisphere. N is the number of structural features of this type used in stereograms.

(a)

(b)
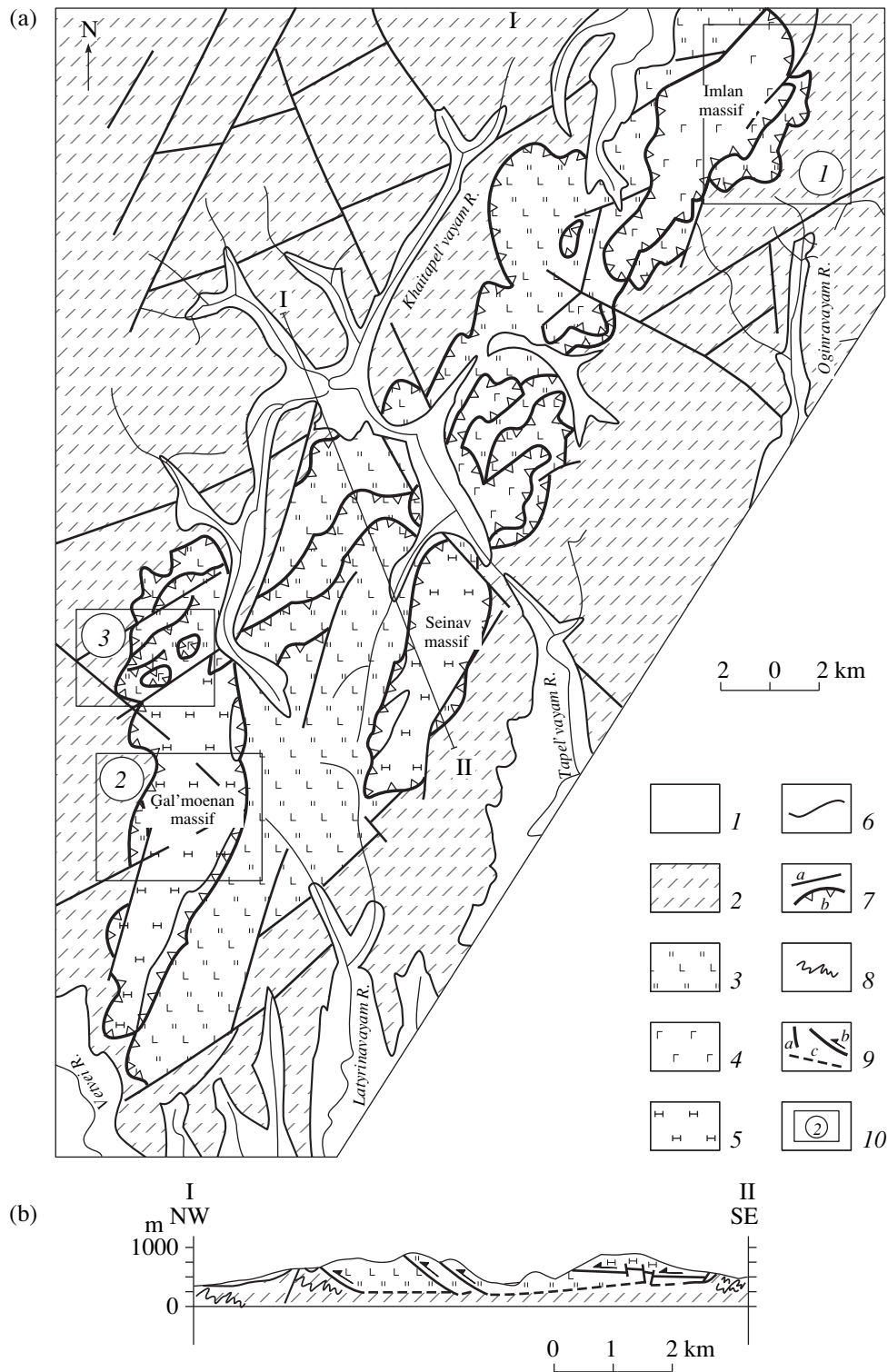
Fig. 6. Schematic geologic map of the Tapelvayam River area. (a) A sector of the State geologic map at a scale of 1 : 200000 (Quad P-58-XXIX), modified after [2]; (b) schematic cross section I–II (modified after [41]). (*1*) Quaternary deposits; (*2*) flyschoid complex of the Ukelayat zone (Coniacian–Lower Eocene); (*3*) volcanic–cherty complex (Campanian–Maastrichtian); (*4*) hyperbasites (Cretaceous?); (*5*) gabbroids (Cretaceous?); (*6*) stratigraphic contacts; (*7*) faulted contacts: high-dipping faults (*a*), thrust faults (*b*); (*8, 9*) on cross section (b): (*8*) folding in the autochthon; (*9*) high-dipping faults (*a*), thrust faults (*b*), the inferred Vatyn-Lesnaya thrust fault surface (*c*); (*10*) site numbers. See Fig. 1b for location.
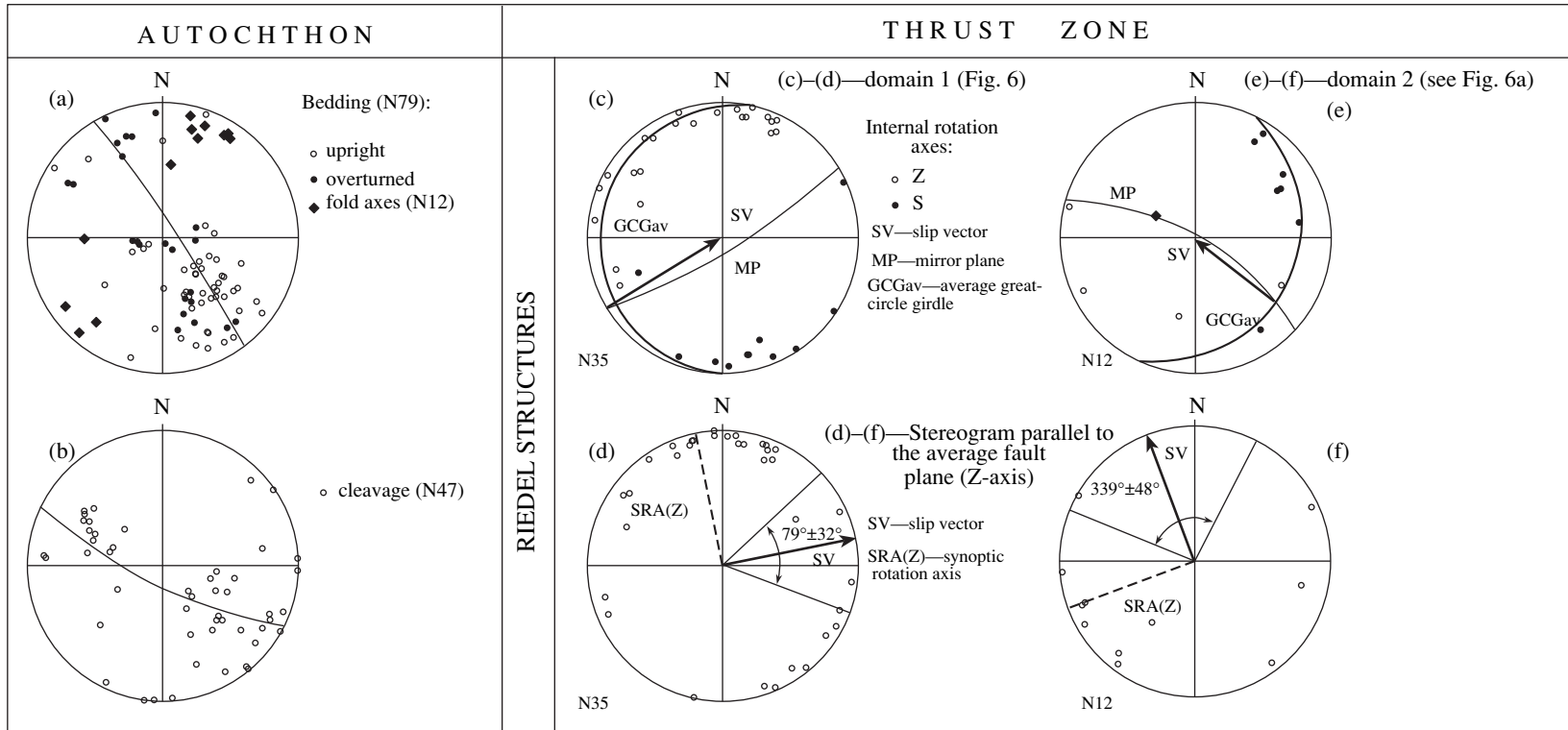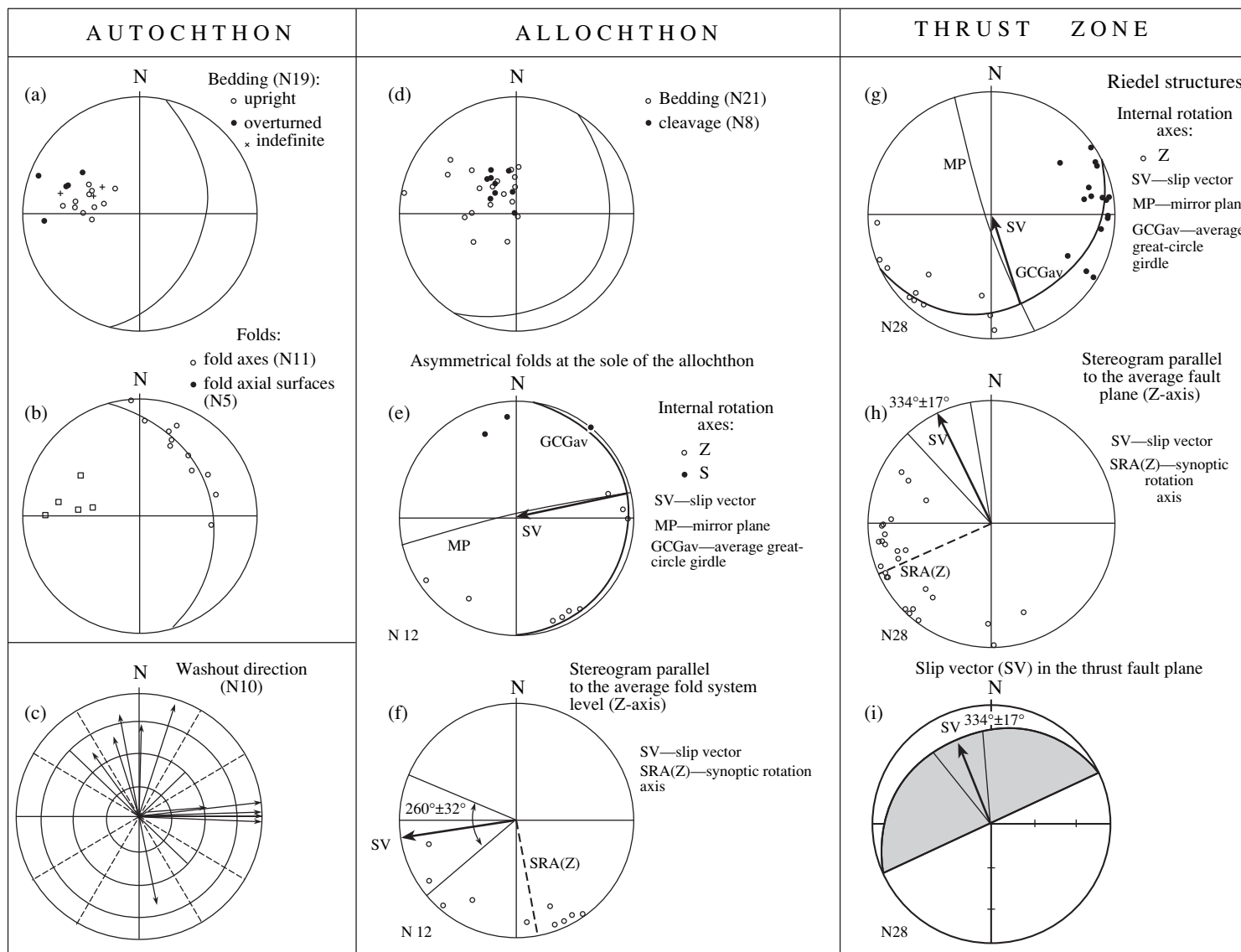
Fig. 7. Structural–kinematic analysis data for the Vatyn–Lesnaya thrust fault (Tapel'vayam River area, see Fig. 6). (a)–(f) stereograms: (a) bedding and β-axes of folds; (b) cleavage, (c)–(f) kinematic analysis in the thrust fault zone: (c), (d) for domain 1; (e), (f) for domain 2 (Fig. 6a): (c), (e) internal rotation axes for Riedel structures, (d), (f) Z-transformed rotation axes for Riedel structures projected at the average fault plane; SV—slip vector; the arc shows the confidence angle. Linear and planar features are shown as poles on the Schmidt net, lower hemisphere. N is the number of structural features of this type used in stereograms.
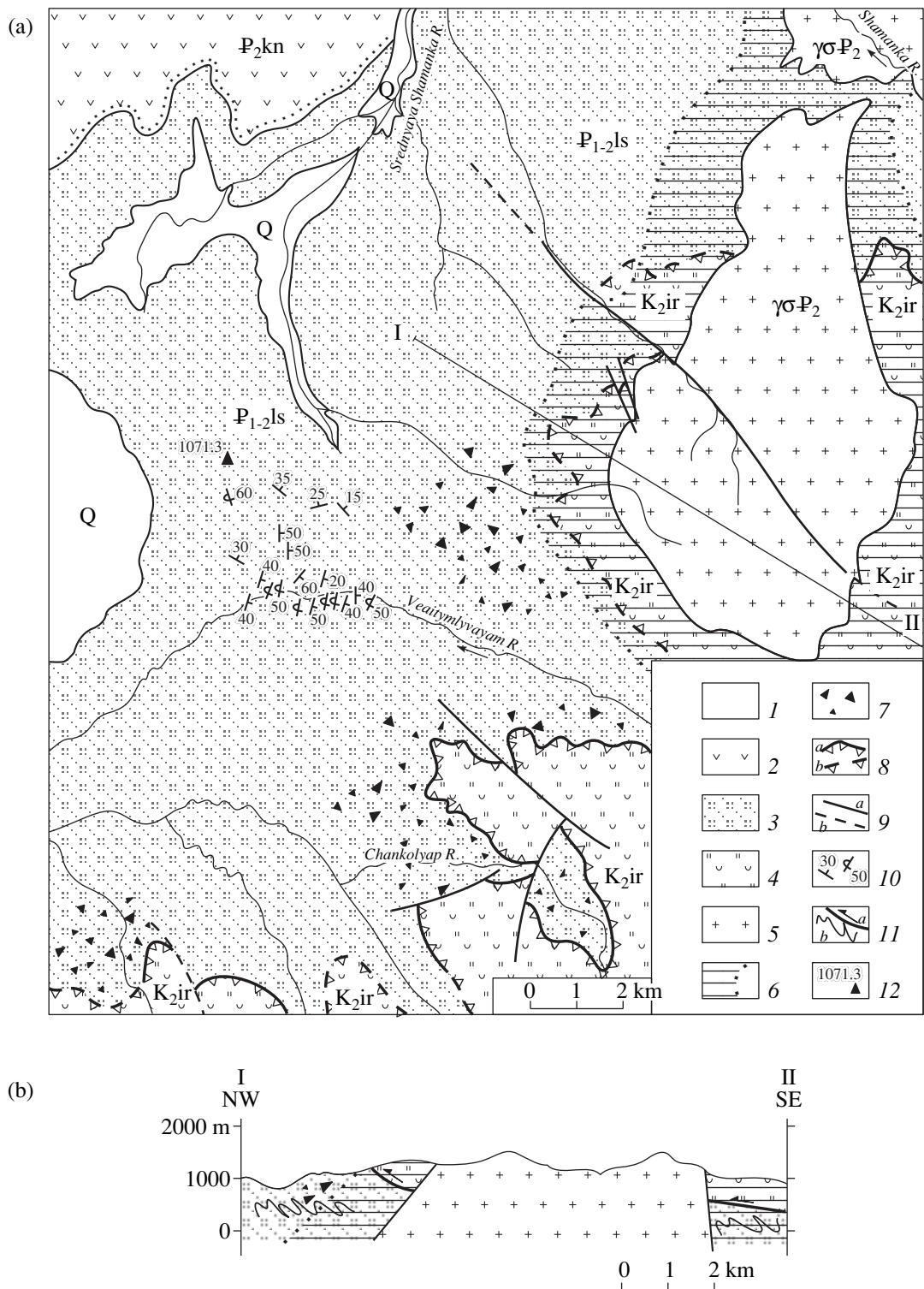
Fig. 8. Structure of the western and southwestern surroundings of the Shamanka granitoid massif [31, 34]: (a) Schematic geologic map, (b) schematic cross section I–II. (*1*) Quaternary deposits; (*2*) Kinkil' Formation (Middle Eocene); (*3*) Lesnaya Group (Pale-ocene–Middle Eocene); (*4*) Irunei Formation (Santonian–Maastrichtian); (*5*) granodiorites; (*6*) hornfels zone and its outer boundary; (*7*) the widest mélange fields in the autochthon of the Lesnaya thrust fault; (*8*) Lesnaya thrust fault: (*a*) mapped, (*b*) inferred in the hornfels field; (*9*) other faults: (*a*) mapped, (*b*) inferred; (*10*) strike and dip symbols; (*11*) in cross section, Fig. 8b: (*a*) Lesnaya thrust fault plane, (*b*) folds in the autochthon; (*12*) elevation in meters. See Fig. 1b for location.
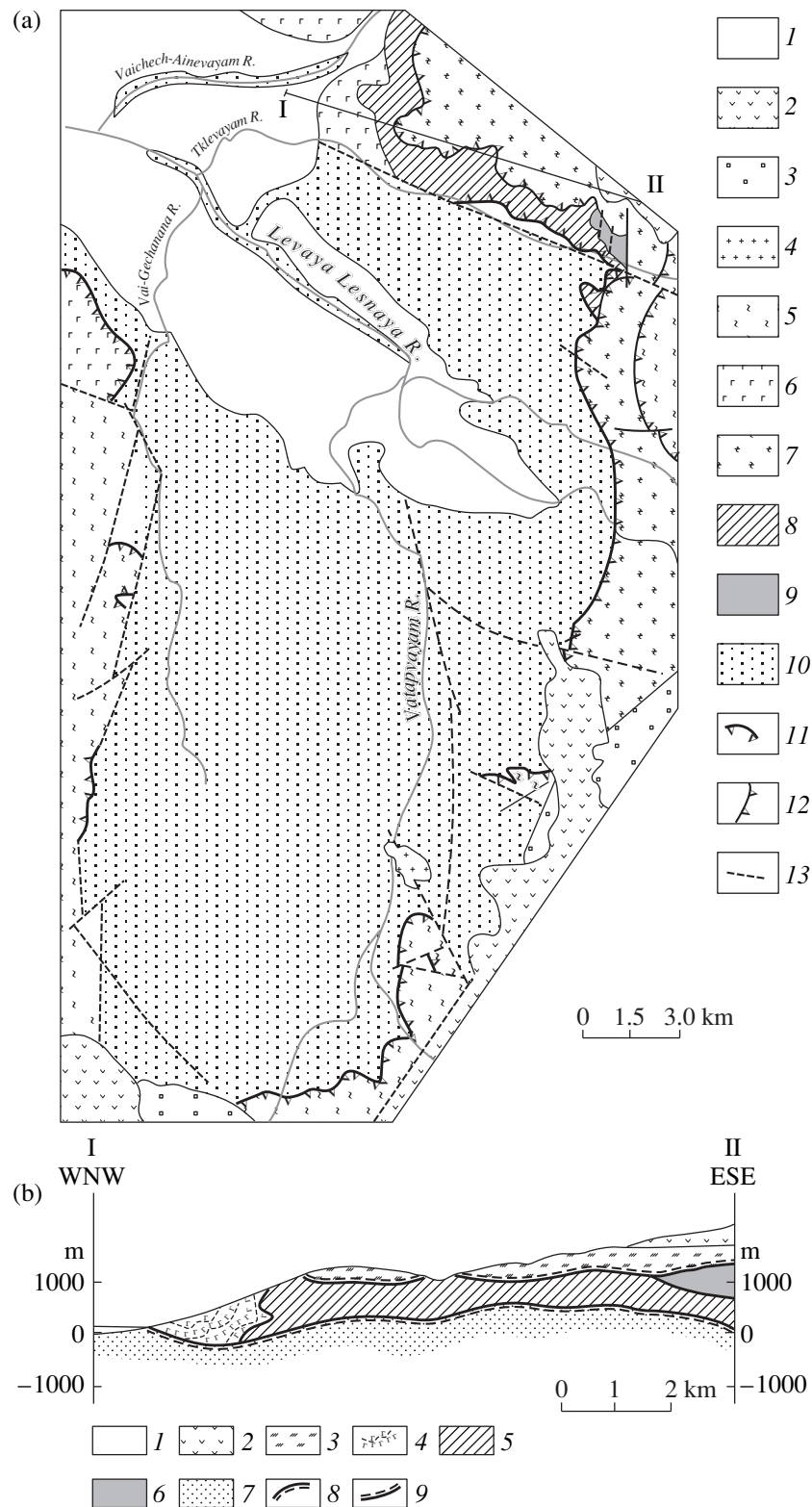
Fig. 9. Schematic geologic map of the Vatapvayam dome [33] (a) and schematic cross section I–II (b). (a): (*1–4*) neoautochthon: (*1*) Quaternary alluvium, (*2*) Miocene–Pliocene subaerial volcanics, (*3*) Middle Eocene, Snatol Formation (shelf sediments), (*4*) Miocene granodiorites; (*5–9*) allochthon: (*5, 6*) Campanian–Maastrichtian, Irunei Formation: (*5*) upper tuff and chert member and (*6*) lower pillow-basalt member; (*7*) greenschists and quartzites (age unknown); (*8*) gabbroids; (*9*) peridotites; (*10*) autochthon: Paleocene–Middle Eocene, Lesnaya Group (clastic flysch); (*11*) Lesnaya thrust fault; (*12*) other faults; (*13*) high-dipping faults. (b): (*1*) Quaternary alluvium; (*2*) Miocene–Pliocene volcanics; (*3*) green schists; (*4*) lower Irunei basalts; (*5*) gabbroids; (*6*) peridotites; (*7*) Lesnaya Group; (*8*) Lesnaya thrust fault; (*9*) sole thrust of the schist sequence. See Fig. 1b for location.

AUTOCHTHON

(a) N

Bedding (N19):
○ upright
● overturned
× indefinite

Folds:
○ fold axes (N11)
● fold axial surfaces (N5)

(b) N

(c) N Washout direction (N10)

ALLOCHTHON

(d) N

○ Bedding (N21)
● cleavage (N8)

Asymmetrical folds at the sole of the allochthon

(e) N

Internal rotation axes:
○ Z
● S

SV—slip vector
MP—mirror plane
GCGav—average great-circle girdle

GCGav

MP SV

N 12

(f) Stereogram parallel to the average fold system level (Z-axis)

N

SV—slip vector
SRA(Z)—synoptic rotation axis

260°±32°

SV

SRA(Z)

N 12

THRUST ZONE

(g) N Riedel structures

Internal rotation axes:
○ Z

SV—slip vector
MP—mirror plane
GCGav—average great-circle girdle

MP

SV

GCGav

N28

(h) Stereogram parallel to the average fault plane (Z-axis)

N

334°±17°

SV

SV—slip vector
SRA(Z)—synoptic rotation axis

SRA(Z)

N28

(i) Slip vector (SV) in the thrust fault plane

N

SV 334°±17°

N28

Fig. 10. Structural–kinematic analysis data for the Lesnaya thrust fault (Shamanka dome, see Fig. 8): (a–i) stereograms: (a) bedding, (b) fold axial surfaces and axes; (c) clastic washout directions reduced to horizontal positions; (d) bedding and cleavage; (e) internal rotation axes for asymmetrical folds; (f) Z-transformed rotation axes for asymmetrical folds projected on the average fold system level; (g–i) kinematic analysis in the thrust fold zone (see Fig. 8a): (g) internal rotation axes for Riedel structures, (h) Z-transformed rotation axes for Riedel structures projected on the average fault plane (SV—slip vector; the arc shows the confidence angle); (i) synoptic slip vector in the Lesnaya thrust fault plane in the study area (see Fig. 8). Linear and planar features are shown as poles on the Schmidt net, lower hemisphere, except (i). N is the number of structural features of this type used in stereograms.

AUTOCHTHON	ALLOCHTHON	THRUST ZONE
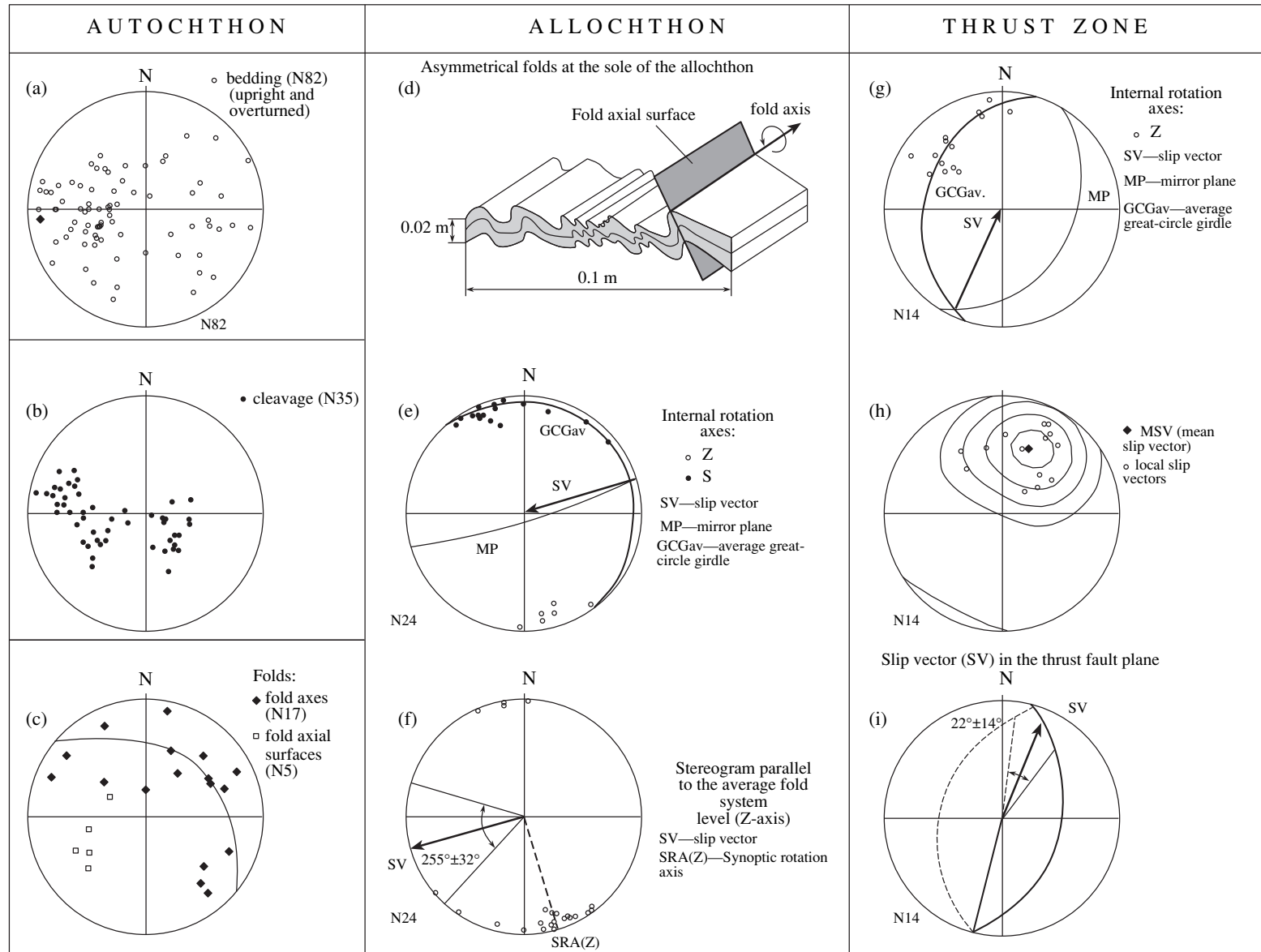
Fig. 11. Structural–kinematic analysis data for the Lesnaya thrust fault (Vatapvayam dome, see Fig. 9). (a)–(c) stereograms: (a) bedding, (b) cleavage, (c) fold axial surfaces and axes; (d) morphology of asymmetrical folds between allochthonous sheets; (e)–(i) stereograms: (e) internal rotation axes for asymmetrical folds; (f) Z-transformed rotation axes for asymmetrical folds projected on the average fold system level; (g)–(i) kinematic analysis in the thrust fault zone (see Fig. 9): (g) internal rotation axes for Riedel structures; (h) dispersion of slip vectors calculated for local Riedel structures; (i) synoptic slip vector on the Lesnaya thrust fault plane in the study area (see Fig. 9). SV—slip vector; the arc shows the confidence angle. Linear and planar features are shown as poles on the Schmidt net, lower hemisphere, except (i). N is the number of structural features of this type used in stereograms.

The surveys in the **Tapel'vayam River basin** were carried out near a large tectonic remnant (Fig. 6) resting upon the flyschoid deposits of the Ukelayat zone, whose age is Coniacian to Early Eocene (87.9 ± 4.5 to 54.8 ± 2.8 Ma as determined by fission-track dating of zircons from sandstones) [38, 39]. The tectonic remnant represents a pile of allochthonous slices composed of Campanian–Maastrichtian volcanic-cherty deposits [24, 41] and hyperbasite-basite rocks. The Vatyn–Lesnaya thrust fault occurs as a zone of mélange with a thickness up to 40 m.

The autochthonous flysch (Fig. 6b) shows isoclinal, predominantly SE-vergent folds (Fig. 7a) with NE- to SW-trending fold axes and axial planar cleavage (Fig. 7b). The Riedel structures in the suprathrust part of the allochthon were studied in two domains. Analysis of these structures suggests that the allochthonous slices (domain 1 in Fig. 6a) were displaced to the east-northeast relative to the allochthon on the eastern slope of the Imlan massif (Figs. 7c, 7d) and to the northwest (Figs. 7e, 7f), on the western slope of the Gal'moenan massif (domains 2 and 3 in Fig. 6a). Note that the estimate of the slip vector is more statistically significant for the former domain than for the latter.

Two domes, Shamanka (Fig. 8) and Vatapvayam (Fig. 9) have been recognized in the **Lesnaya high** on the Kamchatka isthmus. The autochthon of the Lesnaya thrust fault is composed of the Paleocene–Middle Eocene (43.7 ± 3.4 to 58.1 ± 4.2 Ma according to fission-track dating of zircons from sandstones and nanoplankton identified by E.A. Shcherbinina) flysch of the Lesnaya Group [23, 34]. Immediatelly below the Lesnaya thrust plane lies a mélange zone with numerous tuff, sandstone, chert, and basalt blocks. The Late Cretaceous inorceramids and radiolarians were collected from chert blocks [7]. The clastic blocks were dated as Santonian–Campanian based on nanoplankton [34]. The age of the youngest zircon population in them is 86.1 ± 6.1 Ma [A.V. Solov'ev, unpublished]. The allochthon consists largely of Late Cretaceous (Santonian–Maastrichtian) cherty volcanics [7]. The allochthon includes monzonite, gabbro, and occasional hyperbasite bodies and greenschist slices of unknown age (Figs. 9a, 9b). The most probable protolith of these schists were cherty volcanics [33].

The allochthon of the Lesnaya thrust fault is a thin slab slightly deformed by later high-dipping faults. The thrusting amplitude in the direction perpendicular to the predominant strike of Cenozoic structures is estimated at 50 km. In the exposed part of the thrust, the modern thickness of the allochthonous slab is roughly equal to the relative relief value and never exceeds 2 km. The thrust plane is discordant to the mesostructures in the autochthon and allochthon. It is traced by a mylonite zone with a thickness ranging from 1–2 to 10–20 m [31, 33].

The neoautochthonous sequence begins with subaerial volcanics of the Kinkil' Formation [7, 8] and,

locally, the Shamanka Formation [31]. The Kinkil' Formation covers both allochthonous rocks and the autochthonous Lesnaya Group. The basal horizons of the Kinkil' Formation were deposited in the Middle Eocene [31]. The Lesnaya thrust zone is cut by the Middle Eocene Shamanka biotite–hornblende granodiorite massif surrounded by a wide hornfels zone developed both in the autochthon and allochthon (Fig. 8). The apophyses of the massif pass into subvolcanic bodies of the Kinkil' Formation [31]. The basal horizons of the Shamanka Formation are abundant in granodiorite and hornfels pebbles. The age of these horizons, according to fossil flora identification, is interpreted as Late Eocene (37–34 Ma) [31].

The autochthonous flyschoid deposits in the Veaitymlyvayam River valley (Shamanka dome) are deformed into W-vergent isoclinal folds (Fig. 10a), whose axial surfaces dip eastward (Fig. 10b). Fold axes occur along the great-circle girdle and show a northward to eastward strike (Fig. 10b). The observed kinematic indicators (lingulate hieroglyphs and asymmetrical microdunes) suggest a northward and eastward washout of clastics (Fig. 10c). The allochthon structure was investigated on the bluffs of the Chankolyap Creek (Fig. 8). Bedding planes in cherts dip southeastward; cleavage in cherty siltstones is usually oblique to bedding and dips south-southeastward (Fig. 10d). Local asymmetrical microfolds (limb span 1–3 cm) in the allochthonous cherts immediately above the thrust plane suggest a relative westward slip (Figs. 10e, 10f). Analysis of the Riedel structures, widespread in the lower part of the allochthon, suggests that regional transport of the allochthonous complexes relative to the autochthon was northwestward (Figs. 10g, 10h).

Structural surveys were performed in the southwestern and northeastern parts of the Vatapvayam dome (Fig. 9) [33]. The autochthonous flysch is deformed into predominantly west-vergent isoclinal folds (Fig. 11a), the axial surfaces of folds dip to the east-northeast, and fold axes are dispersed along the great-circle girdle and show a NW–SE strike (Fig. 11c). The axial cleavage is widely developed (Fig. 11b). Subhorizontal zones of minor asymmetrical folds, indicative of the westward slip of the allochthonous slabs relative to each other (Figs. 11d–11f), have been recorded in the northeastern part of the dome (Figs. 9a, 9b) at the boundary between the slices composed of gabbros and greenschists. The Lesnaya thrust fault shows a fairly high dip angle in the southeastern part of the dome; in this locality, the Riedel structures in subthrust mylonites indicate a north-northeastward transport (Figs. 11g–11i) [33].

DISCUSSION

The results of the structural–kinematic surveys in various parts of the Vatyn–Lesnaya thrust fault are summarized in the table and in Fig. 1b.

Structure of the allochthon. The allochthon of the Vatyn–Lesnaya thrust fault is a multiply deformed nappe pile [4, 5, 19], but mesoscale folds are scarce within it. Near Anastasia Bay, the allochthon occurs as a synform with a NW- to SE-trending axis (see Fig. 3b, table); in the Il'pi–Vatyn interfluve, the allochthon exhibits wide E- to W-trending synforms alternating with narrow north-vergent antiforms [3]; and in the middle course of the Vyvenka River, we recognized two generations of N–S and SW–NE trending folds in the allochthon [3]. On the Lesnaya high, large folds in the allochthon are generally NE-trending [33], and minor asymmetrical folds between the allochthonous slabs and at the sole of the allochthon show westward vergence (Fig. 1b, table). In all likelihood, the strike of large folds in the allochthon is generally parallel to the Vatyn–Lesnaya thrust plane and repeats its configuration in plan view.

Inner structure of the thrust zone. The slip vectors of the allochthon relative to the autochthon, calculated from Riedel structures in the Vatyn–Lesnaya thrust fault, are directed northward (on the average) but show a wide span of directions (Fig. 1b, table). In three localities, the slip direction was estimated as northeastward, and in the other two, as northwestward. This is probably due to the complex evolution of this collisional suture, where northwestward thrusting across the thrust plane was locally combined with left-slip northeastward movement along the thrust plane [21].

Structure of the autochthon. In all outcrops, the Vatyn–Lesnaya thrust plane is underlain by a tectonized mélange [18, 31, 33] with a sandstone–mudstone matrix (crushed rocks of the Ukelayat and Lesnaya groups) including numerous chert, tuff, basalt, and sandstone blocks, which are just partially correlatable with the overriding allochthon.

The clastic sequence below the mélange zone is deformed into isoclinal folds, whose axes are parallel to the general strike of the Vatyn–Lesnaya thrust fault and the Ukelayat–Lesnaya zone as a whole. Immediately below the thrust plane, these folds usually show a vergence corresponding to the anticipated allochthon transport direction (westward on the Lesnaya high (Figs. 1, 8b, 9b) and north-northeastward in the subthrust zone exposed in the area of the Il'pi and Matysken Rivers (Figs. 1, 4b). At a certain distance from the thrust line, however, the folds in the Ukelayat–Lesnaya zone are inclined toward the thrust fault. This tilt was observed in the Anastasia Bay area (south-southwestward, see Figs. 1, 3b) and in the Tapel'vayam River area (southeastward, see Figs. 1, 6b). The folds in a clastic sequence of Cape Omgon (Omgon Group), lithologically similar to the Lesnaya Group, are also characterized by southeastward vergence (A.V. Solov'ev, unpublished data). The southward and southeastward vergence of structures in the northern surroundings of the Ukelayat trough were reported in [1, 9, 12, 17, 18, 29]. According to our field data, the vergence of structures

depends not only on their position relative to the Vatyn–Lesnaya thrust fault, but also upon the age of the deformed strata.

The stratigraphic subdivision of the flysch sequences in the Ukelayat–Lesnaya trough is insufficiently detailed, because these sequences are strongly deformed. The datings of the flysch complex are based largely on sporadic identified fossil fauna finds [7, 11, 34]. The recently introduced fission-track dating of zircons from sandstones enabled the dating of flysch in four domains located along the Vatyn–Lesnaya thrust fault [21, 23, 38, 39]. Joint analysis of the structural features and ages of these deposits indicates a correlation between them. The vergence of structures in the autochthon, which coincides with the regional vergence of the thrust fault, is typical of the domains (Fig. 4 in the subthrust zone; Figs. 8, 9) composed predominantly of Upper Paleocene-Eocene rocks. The vergence of predominantly Cretaceous–Early Paleocene strata, on the contrary, is opposite to that of the thrust fault (Figs. 6, 3, 4 at a distance from the thrust fault).

According to the published data [12, 30], the age of the flysch in the Ukelayat trough increases northwestward, and the northwestern part of the Ukelayat trough is characterized by predominantly southeastward vergence [1].

To summarize, the Cretaceous–Lower Paleocene strata of the Ukelayat–Lesnaya trough are predominantly vergent toward the Vatyn–Lesnaya thrust; it follows that the deformations in these strata are most probably related to the precollisional evolution of the flyschoid trough. At the same time, the Upper Paleocene–Eocene deposits are deformed conformably with the Vatyn–Lesnaya thrust fault, and, therefore, these folds are syncollisional.

The structural evolution of the Vatyn–Lesnaya suture is closely related to the drift kinematics of the Cretaceous island-arc system relative to northeast Asia. From the Campanian to mid-Paleocene, the arc was an active suprasubduction oceanic structure and drifted rapidly northwestward towards the continent [32, 37]. In the mid-Paleocene (about 60 Ma), the cessation of volcanic activity within the arc was accompanied by flysch accumulation in its southern part sourced from the Eurasian continent [32]. This means that the Ukelayat–Lesnaya basin that separated the arc from the continent was not more than several hundred kilometers in width at that time. However, no significant deformations took place in southern Koryakia and northern Kamchatka in the mid-Paleocene. They are only recorded for the Middle Eocene (about 45 Ma) and contributed to a collision event [26, 34]. In all probability, the arc approached the continent slowly during 15 Ma (from 60 up to 45 Ma). The convergence was compensated by deformations in the arch and, primarily, by the subduction of the Ukelayat–Lesnaya basin floor beneath the continent, which gave rise to south and southeast-vergent (opposite to the Vatyn–Lesnaya thrust fault)

Summary of structural data for the Vatyn–Lesnaya suture zone

Complex Area	Autochthon			Allochthon			Thrust zone		
	Age	Type of structures; vergence	Compression axis orientation	Age	Type of structures; vergence	Compression axis orientation	Type of structures	Slip vector	Compression axis orientation
Anastasia Bay	$K_{2(?)}$–P_2^2 [38, 39]	Folds; SSW	SSW–NNE	$K_{2Tur–Maa}$ [25]	Folds; NE	SW–NE	?	?	?
Il'pi and Matysken rivers	K_{2m}–P_2^2 [38, 39]	Folds, cutoff structures (16° ± 45°, NNE; 196° ± 45°, SSW); fan-folding[1]	SSW–NNE	$K_{2Cmp–Maa}$ [24]	?	?	Riedel structures	38° ± 30°	SW–NE
Tapel'vayam River	K_{2k}–P_2^1 [38, 39]	Folds; SE	SE–NW	$K_{2San–Cmp}$ [41, 24]	?	?	Riedel structures	79° ± 32° (domain 1 in Fig. 6) 339° ± 48° (domain 2 in Fig. 6)	WSW–ENE SE–NW
Lesnaya high (Shamanka dome)	P_2^1 [26]	Folds; W	E–W	$K_{2San–Cmp}$ [7]	Asymmetrical microfolds between allochthonous sheets; W	E–W	Riedel structures	334° ± 17°	SE–NW
Lesnaya high (Vatapvayam dome)	P_1^2–P_2^2 [23, 29]	Folds; W	E–W	$K_{2San–Cmp}$ [7]	Asymmetrical microfolds in the suprathrust part of the allochthon; W	E–W	Riedel structures	22° ± 14°	SSW–NNE

[1] The north-northeastward vergence in the subthrust autochthon passes through fan-folding zone into south-southwestward vergence with distance from the thrust fault.
Question marks indicate the absence of data for this area.

folds in the Cretaceous–Lower Paleocene marine sediments. Underthrusting is probably responsible for the small-scale Paleocene–Early Eocene volcanic eruptions in westernmost Kamchatka and for the accumulation of the Paleocene molasse here [7, 16]. In the mid-Eocene, the relic of this basin was finally closed, and the emplacement of the northwest-vergent Lesnaya thrust took place, which discordantly cut the earlier structures in the arc and continental margin.

CONCLUSION

(1) The Vatyn–Lesnaya thrust fault in the areas studied occurs as a flat, slightly deformed surface separating the lithologically and structurally contrasting autochthonous and allochthonous complexes. As established on the Lesnaya high, this thrust fault was emplaced rapidly, in less than 1 Ma, in the middle Lutetian Age [26, 34]. Data on Riedel structures in the thrust zone suggest that the northwestward thrusting of allochthonous masses was occasionally accompanied by transpressional left-lateral strike-slip displacements.

(2) The allochthonous complex consists of nappes often conjugate with relatively steep imbricated zones. Some allochthonous structures were formed at a great depth sufficient for greenschist metamorphism in the Upper Cretaceous cherty-volcanic sequences. The allochthonous structures were finally formed prior to the mid-Lutetian, considering that the Vatyn–Lesnaya thrust plane is discordant to them.

(3) The autochthonous deposits are deformed into minor isoclinal folds. The folds in the Upper Paleocene–Eocene deposits near the thrust fault exhibit a vergence that coincides with the nappe emplacement direction along the Vatyn–Lesnaya thrust fault—northwestward in the south and northward in the north. At a certain distance from the modern fault line, the Upper Cretaceous–Lower Paleocene strata show folds with an opposite (southward, southeastward) vergence.

(4) Both the autochthon and allochthon of the Vatyn–Lesnaya thrust fault exhibit deformation structures that preceded thrust emplacement. The early deformations in the allochthon are probably related to the initial arc–continent collision, which took place in the mid-Paleocene. From that time, the rapid drift of the paleoarc towards Eurasia gave way to much slower convergence with the continental margin. Deformations in the pre-Upper Paleocene autochthonous strata probably resulted from seafloor subduction beneath the continent [17, 18], which compensated the convergence of the already extinct arc with the continent. The Upper Paleocene–Middle Eocene deposits of the residual Ukelayat–Lesnaya basin remained undisturbed until the Vatyn–Lesnaya thrust emplacement (mid-Lutetian). The thrust emplacement marked the final phase of the collisional event.

REFERENCES

1. Alekseev, E.S., Ocean–Continent Transition Zone Geodynamics with Reference to the Late Mesozoic–Cenozoic Evolution of the Southern Koryak Highland, *Geotektonika,* 1987, no. 4, pp. 102–114.

2. Alekseev, E.S., Kuznetsova, I.A., Lobunets, S.S., and Egorov, I.A., *Geologicheskaya karta SSSR. Vetveiskaya seriya. List P-58-XXIX. Masshtab 1 : 200000* (Geologic Map of the USSR. Vetvei Series. Quad P-58-XXIX. Scale 1 : 200000), Leningrad: Vses. Geol. Inst., 1979.

3. Astrakhantsev, O.V., Geology of the Mafic-Ultramafic Suites of the Olyutorsky Zone (Southern Koryakia), *Abstract of Cand. Sc. (Geol.–Min.) Dissertation*, Moscow, 1996.

4. Astrakhantsev, O.V., Kazimirov, A.D., and Kheifets, A.M., Tectonics of the Northern Olyutorsky Zone, in *Ocherki po geologii Severo-Zapadnogo sektora Tikhookeanskogo tektonicheskogo poyasa* (Essays on the Geology of the Northwestern Pacific Tectonic Belt), Moscow: Nauka, 1987, pp. 161–187.

5. Bogdanov, N.A., Vishnevskaya, V.S., Kepezhinskas, P.K., *et al.*, *Geologiya yuga Koryakskogo nagor'ya* (Geology of the Southern Koryak Highland), Moscow: Nauka, 1987.

6. Bogdanov, N.A. and Kepezhinskas, P.K., Lithospheric Heterogeneity in the Surroundings of the Commander Basin, *Tikhookeanskaya geologiya*, 1988, no. 5, pp. 3–11.

7. *Geologicheskaya karta SSSR. Masshtab 1 : 1000000 (novaya seriya). List Q-57, 58 Palana. Ob"yasnitel'naya zapiska* (Geologic Map of the USSR. Scale 1 : 1000000 (new series). Quad Q-57, 58 Palana. Explanatory Note), Leningrad: Vses. Geol. Inst., 1989.

8. Gladenkov, Yu.B., Sinel'nikova, V.N., Shantser, A.E., Chelebaeva, A.I., *et al.*, *Eotsen Zapadnoi Kamchatki* (The Eocene of Western Kamchatka), Moscow: Nauka, 1991.

9. Grigor'ev, V.N., Krylov, K.A., and Sokolov, S.D., Upper Jurassic–Lower Cretaceous Deposits of the Central Koryak Highland, in *Ocherki po geologii Vostoka SSSR* (Essays on the Geology of the USSR Far East), Moscow: Nauka, 1986.

10. Davis, J.S., *n.p.n.d.* Translated under the title *Statisticheskii analiz dannykh v geologii*, Moscow: Nedra, 1990, 2 vols.

11. Ermakov, B.V. and Suprunenko, O.I., Structure and Depositional Environment of the Late Cretaceous and

Miocene Flysch in the Koryak–Kamchatka Region, *Sov. Geol.*, 1975, no. 12, pp. 53–65.

12. Kazimirov, A.D., Krylov, K.A., and Fedorov, P.I., Tectonic Evolution of Marginal Seas with Reference to the Southern Koryak Highland, *Ocherki po geologii Severo-Zapadnogo sektora Tikhookeanskogo tektonicheskogo poyasa* (Essays on the Geology of the Northwestern Pacific Tectonic Belt), Moscow: Nauka, 1987, pp. 200–225.

13. Kovalenko, D.V., Paleomagnetism and Kinematics of the Central Olyutorsky Range (Koryak Highland), *Geotektonika*, 1996, no. 3, pp. 82–96.

14. Levashova, N.A. and Shapiro, M.N., Paleomagnetism of the Upper Cretaceous Island-Arc Complexes of the Sredinnyi Range in Kamchatka, *Tikhookean. Geol.*, 1999, vol. 18, no. 2, pp. 65–75.

15. Mitrofanov, N.P., Vatyna Nappe in the Central Koryak Fold Zone, *Geol. Geofiz.*, 1977, no. 4, pp. 144–149.

16. *Ob"yasnitel'naya zapiska k tektonicheskoi karte Okhotomorskogo regiona masshtaba 1 : 2 500 000* (Explanatory Note to the Tectonic Map of the Sea of Okhotsk Region, Scale 1 : 2 500 000), Bogdanov, N.A. and Khain, V.E., Eds., Moscow: Ross. Akad. Nauk, 2000.

17. Ruzhentsev, S.V., Byalobzheskii, S.G., Grigor'ev, V.N., Kazimirov, A.D., Peive, A.A., and Sokolov, S.D., Tectonics of the Koryak Range, in *Ocherki tektoniki Koryakskogo nagor'ya* (Essays on the Tectonics of the Koryak Highland), Moscow: Nauka, 1982, pp. 136–189.

18. Sokolov, S.D., *Akkretsionnaya tektonika Koryaksko-Chukotskogo segmenta Tikhookeanskogo poyasa* (Accretionary Tectonics of the Koryak–Chukchi Segment of the Pacific Belt), Moscow: Nauka, 1992.

19. Solov'ev, A.V., Geology and Kinematics of the Vatyn–Vyvenka Thrust (Koryak Highland), *Abstract of Cand. Sc. (Geol.–Min.) Dissertation*, Moscow, 1997.

20. Solov'ev, A.V., Structure of the Northern Junction between the Olyutorsky and Ukelayat Zones (Koryak Highland), *Izv. Vyssh. Uchebn. Zaved. Geol. Razved.*, 1998, no. 3, pp. 23–31.

21. Solov'ev, A.V., Brandon, M.T., Garver, J.I., Bogdanov, N.A., Shapiro, M.N., and Ledneva, G.V., Collision of the Olyutorsky Island Arc with the Eurasian Continental Margin: Kinematic and Age Aspects, *Dokl. Akad. Nauk*, 1998, vol. 360, no. 5, pp. 666–668.

22. Solov'ev, A.V. and Brendon, M.T., Cutoff Method for Kinematic Analysis of Faults in Stratified Sequences, *Geotektonika*, 2000, no. 4, pp. 85–96.

23. Solov'ev, A.V., Garver, J.I., and Shapiro M.N., Fission-Track Ages of Detrital Zircons, *Stratigr. Geol. Korrelyatsiya*, 2001, no. 1, in press.

24. Solov'ev, A.V., Palechek, T.N., and Ledneva, G.V., Campanian–Maastrichtian Deposits of the Frontal Olyutorsky Zone (Southern Koryak Highland), *Stratigr. Geol. Korrelyatsiya*, 2000, vol. 8, no. 2, pp. 88–96.

25. Solov'ev, A.V., Palechek, T.N., and Palechek, R.M., Tectonostratigraphy of the Northern Olyutorsky Zone (Koryak Highland Near Anastasia Bay), *Stratigr. Geol. Korrelyatsiya*, 1998, vol. 6, no. 4, pp. 92–105.

26. Solov'ev, A.V. and Shapiro, M.N., Evaluation of the Emplacement Velocity of the Lesnaya Nappe (Northern Kamchatka), *Materialy konferentsii po issledovaniyam litosfery* (Proc. Conf. on the Studies of the Lithosphere), Moscow: Ross. Akad. Nauk, 2000, pp. 36–38.

27. Stavskii, A.P., Chekhovich, V.D., Kononov, M.V., and Zonenshain, L.P., Plate-Tectonic Palinspastic Models of the Anadyr–Koryak Region, *Geotektonika*, 1988, no. 6, pp. 32–42.

28. Til'man, S.M. and Bogdanov, N.A., *Tektonicheskaya karta Severo-Vostoka Azii. Ob"yasnitel'naya zapiska* (Tectonic Map of NE Asia. Explanatory Note), Moscow: Institut Litosfery AN, 1992.

29. Til'man, S.M., Byalobzheskii, S.G., and Chekhov, A.D., Tectonics and Evolution of the Koryak Geosynclinal System, in *Ocherki tektoniki Koryakskogo nagor'ya* (Essays on the Tectonics of the Koryak Highland), Moscow: Nauka, 1982, pp. 5–30.

30. Chekhovich, V.D., *Tektonika i geodinamika skladchatogo obramleniya malykh okeanicheskikh basseinov* (Tectonics and Geodynamics of the Folded Surroundings of Minor Oceanic Basins), Moscow: Nauka, 1993.

31. Shantser, A.E., Shapiro, M.N., Koloskov, A.V., Chelebaeva, A.I., and Sinel'nikova, V.N., Cenozoic Structural Evolution of the Lesnaya High and Adjacent Territories (Northern Kamchatka), *Tikhookean. Geol.*, 1985, no. 4, pp. 66–74.

32. Shapiro, M.N., Late Cretaceous Achaivayam-Valagin Volcanic Arc (Kamchatka) and North Pacific Plate Kinematics, *Geotektonika*, 1995, no. 1, pp. 58–70.

33. Shapiro, M.N. and Solov'ev, A.V., Structure and Evolution of the Lesnaya Thrust (Severnaya Kamchatka), *Tikhookean. Geol.*, 1999, vol. 18, no. 6, pp. 71–82.

34. Shapiro, M.N., Solov'ev, A.V., Shcherbinina, E.A., Kravchenko-Berezhnoi, I.R., and Garver, J.I., New Data on the Age of the Lesnaya Group in Kamchatka: The Arc–Continent Collision Dating, *Geol. Geofiz.*, 2001, vol. 42, no. 5, pp. 841–851.

35. Cooper, A.K., Marlow, M.S., and Scholl, D.W., Geological Framework of the Bering Sea Crust, in *Geology and Resource Potential of the Continental Margin of Western North America and Adjacent Ocean Basins - Beaufort Sea to Baja California*, Scholl, D.V., Grantz, A., and Vedder J.G., Eds., Houston: Circum-Pacifc Council for Energy and Mineral Resources, Earth Science Series, 1987, vol. 6, pp. 73–102.

36. Cowan, D.S. and Brandon, M.T., A Symmetry-Based Method for Kinematic Analysis of Large-Slip Brittle Fault Zones, *Am. J. Sci.*, 1994, vol. 294, pp. 257–306.

37. Engebretson, D.C., Cox, A., and Gordon, R., Relative Motions Between Oceanic and Continental Plates in the Pacific Basin, *Geological Society of America. Special Paper*, 1985, vol. 206.

38. Garver, J.I., Bullen, M.E., Brandon, M.T., Soloviev, A.V., Ledneva, G.V., and Bogdanov, N.A., Age and Thermal History of the Ukelayet Flysch and Its Bearing on the Timing of Collision of the Olutorsky Terrane, Northern Kamchatka, Russian Far East, *6th International Zoneshain Conference, Moscow, Russia*, Moscow: Geomar, 1998, pp. 173–174.

39. Garver, J.I., Soloviev, A.V., Bulen, M.E., and Brandon, M.T., Towards a More Complete Record of Magmatism and Exhumation in Continental Arcs, Using Detrital Fission-Track Thermochronometry, *Physics and*

Chemistry of the Earth. Part A, 2000, vol. 25, no. 6/7, pp. 565–570.

40. Geist, E.L., Vallier, T.L., and Scholl, D.W., Origin, Transport, and Emplacement of an Exotic Island-Arc Terrane Exposed in Eastern Kamchatka, Russia, *Geol. Soc. of Am. Bull*, 1994, vol. 106, no. 9, pp. 1182–1194.

41. Kravchenko-Berezhnoy, I.R., Ledneva, G.V., Ivanova, E.A., and Vishnevskaya, V.S., Allochthonous Lithotectonic Units of the NW Olutor Terrane (NE Kamchatka), *Ofioliti*, 1993, vol. 18, no. 2, pp. 177–180.

42. Logan, J.M., Friedman, M., Higgs, N., Dengo, C., and Shimamoto, T., Experimental Studies of Simulated Gouge and Their Application to Studies of Natural Fault Zones, *Proceeding of Conference VIII on Analysis of Actual Fault Zones in Bedrock. U.S. Geological Survey. Open-File Report. 9-1239*, 1979, pp. 305–343.

43. Mardia, K.V., *Statistics of Directional Data*, London: Academic Press Ltd, 1972.

44. Ramsay, J.G. and Huber, M.I., *The Techniques of Modern Structural Geology. Vol. 2: Fold and Fractures*, London: Academic, 1987.

45. Robin, P.-Y.F. and Jowett, E.C., Computerized Density Controuring and Statistical Evaluation of Orientation Data Using Counting Circles and Continuous Weighting Functions, *Tectonophysics*, 1986, vol. 121, pp. 207–223.

46. Suppe, J., *Principles of Structural Geology. Englewood Cliffs*, London: Prentice-Hall, Inc., 1985.

47. Twiss, R.J. and Gefell, N.J., Curved Slickenfiber: a New Brittle Shear Sense Indicator with Application to a Sheared Serpentinite, *J. Struct. Geol.*, 1990, vol. 12, pp. 471–481.

48. Worrall, D.M., Tectonic History of the Bering Sea and the Evolution of the Tertiary Strike-Slip Basins of the Bering Shelf, *Geological Society of America. Special Paper*, 1991, vol. 257.

Reviewers: S.D. Sokolov, N.A. Bogdanov, and M.L. Kopp